Theoretical Calculations on the Cycloreversion of Oxetane Radical Cations

M. Angeles Izquierdo,[†] Luis R. Domingo,*[,‡] and Miguel A. Miranda*[,†]

Departamento de Química Orgánica/Instituto de Ciencia Molecular, Universidad de Valencia, c/Dr. Moliner 50, 64100, Valencia, Spain, and Departamento de Química/Instituto de Tecnología Química UPV-CSIC, Universidad Politécnica de Valencia, Camino Vera s/n, Apdo. 22012, 46022, Valencia, Spain

Received: September 15, 2004; In Final Form: January 21, 2005

The molecular mechanism for the cycloreversion of oxetane radical cations has been studied at the UB3LYP/6-31G* level. Calculations support that the cycloreversion takes place via a concerted but asynchronous process, where C−C bond breaking at the transition state is more advanced than O−C breaking. This allows a favorable rearrangement of the spin electron density from the oxetane radical cation (with the spin density located mainly on the oxygen atom) to the alkene radical cation which is one of the final products. Inclusion of solvent effects does not modify the gas-phase results.

Oxetanes can be easily obtained by Paterno−Büchi photocycloaddition of carbonyl compounds to alkenes.[1] Their cycloreversion (CR) involves cleavage of two bonds and may yield formal methathesis products.[2] This process can be achieved by using electron transfer (ET) photosensitizers and has recently attracted considerable interest, as it appears to be involved in the photorepair of DNA.[3]

In a previous study, semiempirical calculations were used to study the ET-catalyzed CR of the oxetanes proposed as intermediates in the photoenzymatic repair of (6-4) photoproducts of DNA dipyrimidine sites by photolyases.[4] The stationary points on the potential energy surfaces for the gas-phase splitting were located by AM1 and PM3 methods. These calculations showed that cleavage of the radical anions is more exothermic than that of the radical cations. A nonconcerted, two-step mechanism was proposed for both radical anion and radical cation pathways at these semiempirical levels. In the oxidative ET cycloreversion, initial C−C bond cleavage is favored (Scheme 1, pathway $b_1 + b_3$); by contrast, the reductive pathway appears to start with C−O breaking.

There are no experimental data in the literature related to the CR of simple oxetanes such as **1a** and **1b** (Chart 1). However, CR of 2,2-diaryloxetanes using cyanoaromatics as ET photosensitizers[5] was proposed to follow the mechanism predicted by semiempirical calculations, based on the stereochemistry of the products. Thus, CR would occur with cleavage of the same bonds (C_2-C_3 and C_4-O) formed in the synthesis of the oxetanes. Although the process was explained via formation of radical cations, no intermediate of this type was detected.

The same regioselectivity has been observed in recent experiments performed in our group on the CR of the model compound *trans,trans*-2,3-diphenyl-4-methyloxetane (**1c**) mediated by chloranil (**2**);[6] the obtained products are those resulting from addition of $\mathbf{2}^{\bullet-}$ or $\mathbf{2H}^{\bullet}$ to the *trans*-β-methylstyrene radical cation.

SCHEME 1

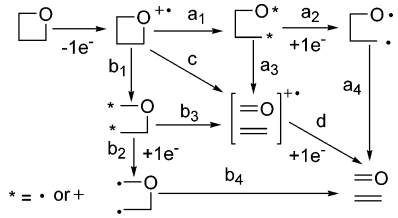

CHART 1

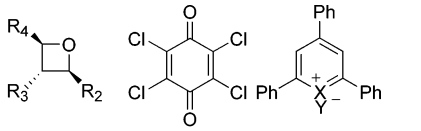

1a $R^2 = R^3 = R^4 = H$ **2** **3a**: X = O, Y = BF_4
1b $R^2 = R^3 = R^4 = Me$ **3b**: X = S, Y = OCl_4
1c $R^2 = R^3 = Ph$, $R^4 = Me$
1d $R^2 = R^3 = Ph$, $R^4 = CH_2OH$

It is remarkable that the regioselectivity of ET-mediated CR of oxetanes can be controlled by modifying the nature of the photosensitizer.[6] Thus, we have found that CR of **1c** using 2,4,6-triaryl(thia)pyrylium salts (**3a,b**) as alternative photosensitizers occurs with initial $O-C_2$ bond cleavage.[7] In the resulting 1,4-radical cation, spin and charge are located in the oxygen and C_2 atoms, respectively. Subsequent C_3-C_4 bond cleavage results in the production of *trans*-stilbene and acetaldehyde (Scheme 1, pathway $a_1 + a_3$). This mechanism is supported by intramolecular trapping of the cationic site in the partially cleaved intermediate in the case of the hydroxymethyl substituted oxetane **1d**. The relevant transient species (*trans*-stilbene radical cation and pyranyl radical) have been detected by means of laser flash photolysis (LFP) of **1c** and **1d** in the presence of (thia)-pyrylium salts.

The results obtained using cyanoaromatics[5] and chloranil[6] as photosensitizers agree with predictions;[4] by contrast, those obtained using (thia)pyrylium salts as photosensitizers[7] cannot be explained according to this model. With this background, it appeared interesting to perform theoretical calculations on the splitting mode of oxetane radical cations, using model com-

* To whom correspondence should be addressed. E-mail: domingo@utopia.uv.es, mmiranda@qim.upv.es.
† Departamento de Química/Instituto de Tecnología Química UPV-CSIC, Universidad Politécnica de Valencia.
‡ Departamento de Química Orgánica/Instituto de Ciencia Molecular, Universidad de Valencia.

10.1021/jp045832o CCC: $30.25
Published on Web 03/02/2005

TABLE 1: Total Energies (in au) and Relative Energies[a] (in kcal/mol, in Parentheses, Relative to the Corresponding Oxetane Radical Cations) for the Stationary Points along the CR of $1a^{\bullet+}$, $1b^{\bullet+}$, and $1c^{\bullet+}$

species		UB3LYP/6-31G*		MP2/6-31G*		MP3/6-31G*//MP2/6-31G*		UB3LYP/6-31G* (acetonitrile)	
1a	**RC**	−192.764030		−192.118751		−192.156172		−192.847667	
	TS-CC	−192.741323	(14.5)	−192.104921	(8.3)	−192.132903	(14.2)	−192.824759	(14.6)
	TS-OC	−192.708907	(32.9)	−192.068457	(29.8)	−192.095895	(36.0)	−192.795664	(30.9)
	MC	−192.768182	(−3.1)	−192.138928	(−13.5)	−192.166245	(−7.2)	−192.846303	(0.4)
1b	**RC**	−310.742242						−310.813230	
	TS-CC	−310.741916	(0.5)					−310.814299	(−0.4)
	TS-OC	−310.706647	(20.8)					−310.781661	(18.3)
	MC	−310.770486	(−19.7)					−310.837374	(−17.1)
1c	**RC**	−694.258389						−694.318937	
	TS-CC	−694.240016	(10.9)					−694.305262	(7.9)
	TS-OC	−694.221296	(22.2)					−694.282967	(21.5)
	MC	−694.302074	(−29.2)					−694.353310	(−23.3)

[a] Relative energies including zero point energies (ZPE).

pounds more similar to our simple systems. This could allow the use of a density functional theory (DFT) treatment, at a higher level that the previous semiempirical studies. The models selected for the present work have been the parent unsubstituted oxetane radical cation, $\mathbf{1a}^{\bullet+}$, the 2,3,4-trimethyl derivative $\mathbf{1b}^{\bullet+}$, and the 4-methyl-2,3-diphenyl derivative $\mathbf{1c}^{\bullet+}$. For all of them, two reactive channels have been studied, corresponding to the initial O−C or C−C bond breaking process.

Computational Methods. DFT calculations were carried out using the B3LYP[8] exchange-correlation functional, together with the standard 6-31G* basis set.[9] For the studied radical species, the unrestricted formalism (UB3LYP) was employed. In addition, second- and third-order Moller−Plesset theory (MP2 and MP3) calculations[9] were also performed for the smallest system $\mathbf{1a}^{\bullet+}$, to test the reliability of the DFT method. Optimizations were carried out using the Berny analytical gradient optimization method.[10] The stationary points were characterized by frequency calculations, to verify that the transition structures (TSs) have one and only one imaginary frequency. The intrinsic reaction coordinate (IRC)[11] path was traced in order to check the energy profiles connecting each TS with the two associated minima of the proposed mechanism by using the second-order González−Schlegel integration method.[12] The electronic structures of stationary points were analyzed by the natural bond orbital (NBO) method.[13] All calculations were carried out with the Gaussian 98 suite of programs.[14]

The solvent effects on the mechanism of cycloreversion of the selected oxetane radical cations have been considered by UB3LYP/6-31G* optimizations of the gas-phase stationary points, using a relatively simple self-consistent reaction field[15] (SCRF) method based on the polarizable continuum model (PCM) of Tomasi's group.[16] As the solvent used in the experimental work was acetonitrile, we have used its dielectric constant of $\epsilon = 36.64$.

The topological analysis of electron densities was performed by employing Bader's theory of atoms in molecules (AIM).[17] This theory partitions the charge density ($\rho(r)$) of a molecule in a set of nonoverlapping atomic domains whose surface is characterized by a local zero-flux in the gradient vector field of ($\rho(r)$). The Laplacian of charge density, $\nabla^2\rho(r)$, indicates whether the charge being associated with attractors and bond critical points (BCPs) is locally concentrated ($\nabla^2\rho(r) < 0$) or locally depleted ($\nabla^2\rho(r) > 0$).

Results and Discussion

Energies for the Fragmentation of Oxetane Radical Cations. A detailed analysis of the results indicates that this fragmentation takes place along concerted but highly asynchronous processes. Therefore, one oxetane radical cation (**RC**), two **TS**s (namely **TS-OC** and **TS-CC**) and a molecular complex (**MC**) where both fragments of the cycloreversion remain associated have been studied and analyzed in each case (Scheme 2). The total and relative energies are given in Table 1.

SCHEME 2

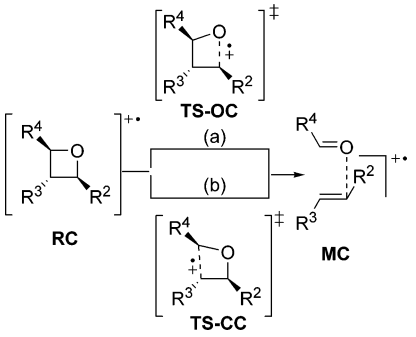

First, the mechanism for the CR of the simplest oxetane radical cation $\mathbf{1a}^{\bullet+}$ was studied in the gas phase at the UB3LYP/6-31G*, MP2/6-31G*, and MP3/6-31G*//MP2/6-31G* levels. These three levels were selected to ascertain whether the DFT results could be suitable for the global study. The activation barriers for fragmentation of $\mathbf{1a}^{\bullet+}$ via **TS-CC** and **TS-OC** were 14.5 and 32.9 kcal/mol (UB3LYP), 8.3 and 29.8 kcal/mol (MP2), or 14.2 and 36.0 kcal/mol (MP3), respectively. At the three computational levels, initial cleavage of the C−C bond is clearly favored over that of the O−C bond. For the more favorable path via **TS-CC**, the MP2 calculations gave a barrier somewhat lower than that found at the DFT level. With MP3, results were similar to those of UB3LYP. Therefore, the DFT computational method was selected to study the cycloreversion of $\mathbf{1b}^{\bullet+}$ and $\mathbf{1c}^{\bullet+}$. At this level, splitting of the simplest model $\mathbf{1a}^{\bullet+}$ is slightly exothermic, −3.1 kcal/mol.

Fragmentation of the trimethyl derivative $\mathbf{1b}^{\bullet+}$ presents a very low barrier when compared with $\mathbf{1a}^{\bullet+}$. Its value along the **TS-CC** channel is as low as 0.5 kcal/mol. Again, this path is less energetic (by ca. 20 kcal/mol) than CR via **TS-OC**. Overall, cycloreversion of $\mathbf{1b}^{\bullet+}$ is strongly exothermic (−19.7 kcal/mol).

The CR for model compounds $\mathbf{1a}^{\bullet+}$ and $\mathbf{1b}^{\bullet+}$ has two degenerated C−C and O−C bond breaking pathways due to the symmetry of the reactants. However, in the case of oxetane $\mathbf{1c}^{\bullet+}$ ring splitting can occur with different regioselectivity, with $O-C_2/C_3-C_4$ or $O-C_4/C_2-C_3$ bond cleavage, as stated in the Introduction. Both possibilities were investigated. In the latter case, oxetane radical cation $\mathbf{1c}^{\bullet+}$ fragments spontaneously through initial C_2-C_3 bond cleavage with an unappreciable barrier. This fact precludes characterization of the corresponding

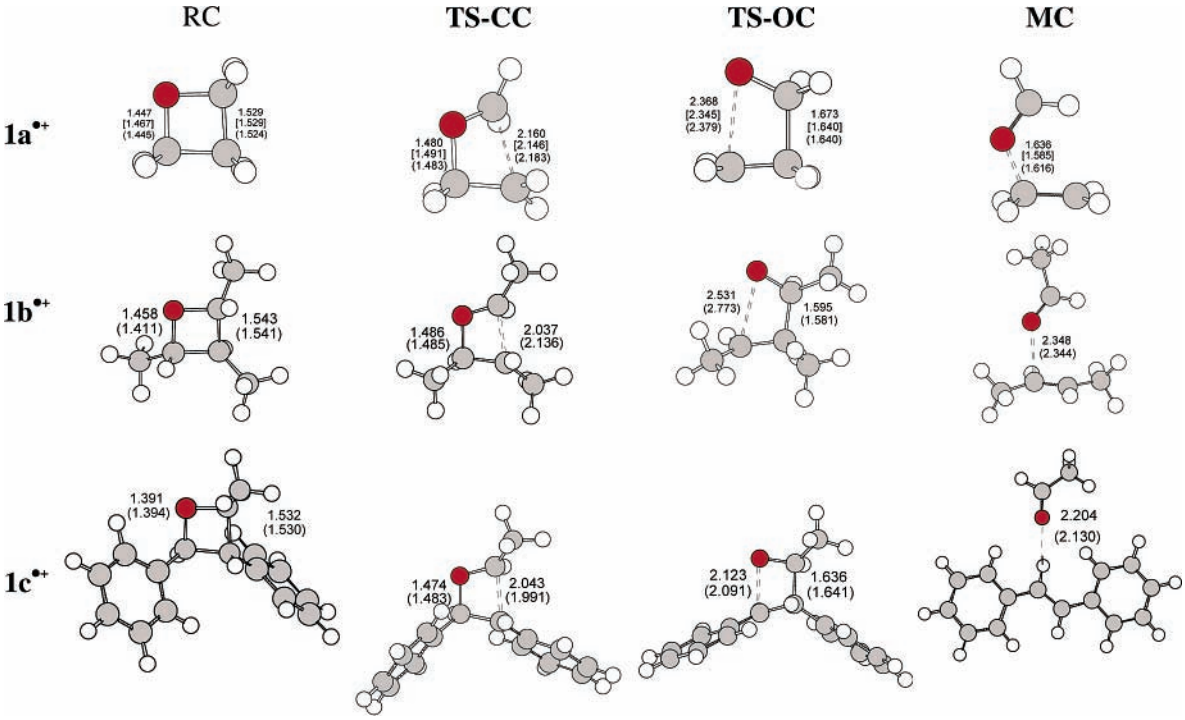

Figure 1. Stationary points corresponding to the cycloreversion of the oxetane radical cations **1a**$^{\bullet+}$, **1b**$^{\bullet+}$, and **1c**$^{\bullet+}$. The bond lengths directly involved in the reaction obtained at UB3LYP/6-31G*, UMP2/6-31G* (in brackets), and SCRF-UB3LYP/6-31G* (in parentheses) are given in angstroms.

TS. When the former pathway was explored, CR of **1c**$^{\bullet+}$ via **TS-CC** presented a barrier of 10.9 kcal/mol, close to that found for **1a**$^{\bullet+}$. The barrier for initial O−C_2 cleavage via **TS-OC** is ca. 12 kcal/mol higher in energy.

As the experimental data on these reactions were obtained in solution, where the solvent effects can have a strong influence on the mechanism, such solvent effects on the CR of the selected oxetane radical cations have also been considered (see Computational Methods). The energetic results are given in Table 1. In acetonitrile, the CR barriers generally decrease in the range 0.1−3.0 kcal/mol, but initial C−C bond breaking still remains favored relative to O−C cleavage.

Geometry of the Stationary Points. The geometries of the stationary points are shown in Figure 1. An analysis of the geometrical parameters of the stationary points for the CR of **1a**$^{\bullet+}$ obtained at the DFT and MP2 levels shows that there are no significant differences.

The lengths of the O−C_2 and C_3−C_4 breaking bonds at the TSs indicate that they are associated with highly asynchronous processes, where breaking of the C_3−C_4 bond at **TS-CC** and the O−C_2 bond breaking at **TS-OC** are more advanced. Inclusion of solvent effects in the geometry optimizations does not modify substantially the gas-phase results.

The geometries of the CR products show that in **MC**s there is a strong interaction between the oxygen atom of the carbonyl compound and the alkene derivative that supports most of the positive charge. In addition, this interaction decreases with increasing substitution of the alkene fragment. Thus, the O−C_2 distances at **MC** (1.636 and 2.348 Å for **1a**$^{\bullet+}$ and **1b**$^{\bullet+}$, respectively) indicate a larger interaction in the former. The geometry of the **MC** obtained from the CR of **1a**$^{\bullet+}$ reveals that the ethylene C_2 carbon atom remains sp^3 hybridized, as a consequence of the large interaction with the lone pair of the oxygen atom. The presence of the two methyl groups on the alkene fragment derived from **1b**$^{\bullet+}$ stabilizes more effectively the alkene radical cation, decreasing the interaction with the carbonyl oxygen atom. This fact is in agreement with the larger exothermic character for the CR of **1b**$^{\bullet+}$. Finally, the alkene radical cation generated from **1c**$^{\bullet+}$ is largely stabilized due to the presence of the two phenyl substituents.

Analysis of the atomic motion along the unique negative vibrational frequency associated with the less energetic **TS-CC** indicates that it is mainly associated with motion of the C_3 and C_4 carbon atoms along the C−C breaking bond, whereas motion of the O and C_2 atoms is negligible. A different behavior is found at the more energetic **TS-OC**, where the C_3 and C_4 atoms have also a large participation. These results, which are in agreement with the bond lengths found at the corresponding TSs, indicate that O−C_2 bond breaking at the more favorable **TS-CC** is more delayed than C_3−C_4 cleavage at **TS-OC**, as a consequence of the large O−C_2 interaction at the former.

In view of the high asynchronicity of the TSs found for these CR processes, specially those associated with initial C−C bond breaking, the IRCs from **TS-CC** and **TS-OC** to **RC** and **MC** were traced. Analysis of the results indicates that O−C and C−C bond breaking after the TSs takes place in a sequential procedure, without the participation of any intermediate. Because of the contour of the IRCs, which does not present any shoulder, the existence of any intermediate associated with a stepwise process can be ruled out.

Bond Order Analysis. The extent of bonding along a reaction pathway is provided by the concept of bond order (BO).[18] The BO values of the O−C_2 and C_3−C_4 breaking bonds at **TS-CC** and **TS-OC** are given in Table 2. An analysis of the BO values of the two breaking bonds at the TSs indicates that they correspond to asynchronous bond breaking processes. At the less energetic **TS-CC**, breaking of the C_3−C_4 bond (BO of ca. 0.4) is more advanced than that of the O−C_2 bond (BO of ca. 0.8), while at **TS-OC** breaking of the O−C_2 bond is very advanced and that of the C_3−C_4 bond is more delayed (see Table 2). At the more favorable **TS-CC**, the O−C BO values are lower than those found in the **RC** (ca. 0.9).

TABLE 2: UB3LYP/6-31G* Wiber Bond Order Values of the O_1-C_2 and C_3-C_4 Breaking Bonds at TS-CC and TS-CO

	TS-CC		TS-OC	
	$O-C_2$	C_3-C_4	$O-C_2$	C_3-C_4
1a$^{\bullet+}$	0.82	0.36	0.06	0.77
1b$^{\bullet+}$	0.81	0.39	0.06	0.88
1c$^{\bullet+}$	0.83	0.40	0.26	0.80

TABLE 3: UB3LYP/6-31G* Total Atomic Spin Densities for the Stationary Points along the Cycloreversion of the Radical Cation of 1a$^{\bullet+}$

atom	RC	TS-CC	TS-OC	MC
O	0.702	0.268	0.909	0.081
C_2	−0.007	−0.045	0.000	0.035
C_3	0.006	0.636	−0.007	0.946
C_4	−0.007	0.129	−0.053	0.004

At this point, it appeared interesting to compare the Wiber indexes with the BOs obtained from the natural resonance theory (NRT). The total bond order values[19] between the $O-C_2$ and C_3-C_4 at the TSs involved in the CR of **1a**$^{\bullet+}$ were found to be 0.99 and 0.48 at **TS-CC** and 0.43 and 0.68 at **TS-OC**, respectively. Thus, the total bond order values at **TS-CC** are close to the Wiber index, whereas at **TS-OC** the total bond order between the $O-C_2$ is very large. In the latter case, the Wiber index is in better agreement with the topological analysis (see below).

Analysis of the Atomic Charges and the Spin. An analysis of the natural atomic charges at the oxetane radical cations **RC** shows that the positive charge is mainly located at the C_2-O-C_4 fragment. This charge distribution results from delocalization of the electron-density of the C_2 and C_4 carbon atoms on the neighboring oxygen atom and accounts for the more favorable C_3-C_4 bond breaking that allows a larger stabilization of the incipient alkene radical cation.

Analysis of the charges at **TS-CC** and **TS-OC** for **1a**$^{\bullet+}$ shows that the alkene fragment supports most of the positive charge, 0.73 and 0.68 au, respectively. The large positive charge found at the less energetic **TS-CC** is a consequence of the strong interaction with the oxygen atom.

Finally, analysis of the total atomic spin densities for the stationary points associated with the cycloreversion of **1a**$^{\bullet+}$ indicates that although in the starting oxetane radical cation **RC** the oxygen atom supports a larger spin density (0.70), in the reaction product **MC** the C_3 atom belonging to ethylene supports the larger spin density (0.95) (see Table 3). For the TSs, while at **TS-OC** the oxygen atom presents a large spin density (0.91), at the more favorable **TS-CC** the spin density at the O and C_3 atoms, 0.27 and 0.64, respectively, shows the logical progress from the reactant to the product.

Bader Topological Analysis. To study the changes in electronic structure along these CR reactions, a topological analysis of the electron density, $\rho(r)$, was performed for the stationary points in the case of **1a**$^{\bullet+}$ using Bader's theory of AIM. The results are summarized in Table 4. In **TS-CC** the electron density at the BCPs between O_1-C_2 and C_3-C_4 was found to be 0.2166 and 0.0556, respectively. Thus, the electron density at the BCP associated with the O_1-C_2 bond is nearly the same as at **RC** (0.2334), while in the case of the C_3-C_4 bond it is largely reduced (as compared with 0.2510 at **RC**). In **TS-OC** the electron density at the BCP between C_3-C_4 is 0.1733, while there is no BCP between the O_1-C_2, indicating that these atoms are not bonded anymore. The symbol $\nabla^2\rho(r)$ shows the properties of the bonding: when $\nabla^2\rho(r) < 0$ it means that the electrons are concentrated between the two atoms so that a covalent bond is formed by sharing the electrons, and when $\nabla^2\rho(r) > 0$ it means that the charge is locally depleted to an atom. At **TS-CC** the $\nabla^2\rho(r)$ values associated with the O_1-C_2, C_2-C_3, and C_4-O_1 bonds are negative, indicating covalent bonds. However, $\nabla^2\rho(r)$ for the C_3-C_4 bond is positive. At **TS-OC** the $\nabla^2\rho(r)$ values associated with the C_2-C_3, C_3-C_4, and C_4-O_1 bonds are negative. It is interesting to remark the topological analysis at **MC**. This species presents a BCP between the O_1-C_2 belonging to the formaldehyde and alkene radical cation frameworks, $\rho(r) = 0.1445$. Finally, **TS-CC** has a ring critical point that means that this TS is still a cyclic system, while **TS-OC** does not have such a point in agreement with an open system.

TABLE 4: UB3LYP/6-31G* Topological Properties (in au) of Electron Density Distribution at the BCPs for the Stationary Points along the Cycloreversion of Radical Cation 1a$^{\bullet+}$

	RC			MC		
bond	$\rho(r)$	$\nabla^2\rho(r)$	ϵ	$\rho(r)$	$\nabla^2\rho(r)$	ϵ
O_1-C_2	0.2334	−0.1846	0.0467	0.1445	−0.0054	0.0859
C_2-C_3	0.2510	−0.5908	0.0337	0.2827	−0.7309	0.0537
C_3-C_4	0.2510	−0.5909	0.0337			
C_4-O_1	0.2335	−0.1841	0.0467	0.3751	0.4024	0.0586
	TS-CC			**TS-OC**		
bond	$\rho(r)$	$\nabla^2\rho(r)$	ϵ	$\rho(r)$	$\nabla^2\rho(r)$	ϵ
O_1-C_2	0.2166	−0.3043	0.0337			
C_2-C_3	0.2632	−0.6533	0.0564	0.3013	−0.8534	0.0849
C_3-C_4	0.0556	0.0790	0.3604	0.1733	−0.2757	0.0247
C_4-O_1	0.3308	−0.1726	0.1444	0.3017	−0.5714	0.1681

This topological analysis reinforces the conclusions about the asynchronicity on the bond breaking process at both TSs based on the Wiber's BO analysis. Thus, in **TS-CC** the O_1-C_2 bond remains with electronic properties similar to those at **RC**, while the C_3-C_4 bond breaking is very advanced but with a bonding character. A different picture is found for **TS-OC** where there is no bonding between O_1-C_2 anymore; the Wiber O_1-C_2 BO at this TS is 0.06.

Discussion

On the basis of the obtained results, the present DFT study for the mechanism of the CR of oxetane radical cations supports a concerted but highly asynchronous process where only the C_3-C_4 bond is being broken at the TS while the O and C_2 atoms still remain bonded. Although previous work on the oxidative ET-CR of more complex oxetanes using semiempirical AM1 and PM3 calculations[4] appeared to support a stepwise pathway, the second TS was found to be only slightly above (0.3 kcal/mol) the reaction intermediate. Thus, taking into account that these semiempirical methods tend to predict stepwise rather than concerted mechanisms, the present findings are not substantially different from the literature results. At the **TS-CC** the positive charge and the spin density are mainly located in the alkene fragment, as stated from the analysis of the charge distribution and the total atomic spin density. These results were consistently the same for all the selected oxetanes, regardless of the method employed for the study and the reaction medium (gas phase or solution).

In the case of *trans,trans*-2,3-diphenyl-4-methyloxetane **1c**$^{\bullet+}$, the transition structure resulting from fragmentation through C_2-C_3 and $O-C_4$ was impossible to optimize because **1c**$^{\bullet+}$

SCHEME 3

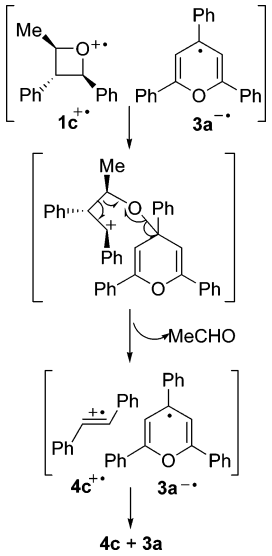

breaks directly to produce β-methylstyrene radical cation and benzaldehyde. This behavior can be explained taking into account the strong hindrance between the two aryl groups and the large stabilization of the resulting products, which favors bond breaking through C_2-C_3. These theoretical results agree with experimental data found in the CR of 2,2-diaryloxetanes and 2,3-diaryloxetanes using cyanoaromatics and chloranil, respectively, as ET-photosensitizers. However, they cannot explain the opposite regioselectivity observed for the CR of **1c,d** photosensitized by (thia)pyrylium salts **3a,b**, that starts with fragmentation of the $O-C_2$ bond.

This different reactivity may be due to the degree of charge separation associated with the electron transfer step. In the case of **2** and cyanoaromatics, after ET, two neutral species give rise to a radical anion plus a radical cation. However, using (thia)-pyrylium salts, a cation plus a neutral compound give rise to a radical plus a radical cation. Taking into account the spin distribution found for the oxetane radical cation $\mathbf{1a}^{\bullet+}$, which is mainly located in the oxygen atom, it would be conceivable that the pyranyl radical interacts with the oxetane radical cation before fragmentation. This would direct the CR pathway, facilitating fragmentation through the $O-C_2$ bond. This possibility is illustrated in Scheme 3.

After electron transfer, the oxygen atom of the oxetane radical cation $\mathbf{1c}^{\bullet+}$ might bond to the radical center of the pyranyl radical. Subsequent bond breaking would give rise to *trans*-stilbene radical cation $\mathbf{4c}^{\bullet+}$ plus pyranyl radical $\mathbf{3a}^{\bullet-}$. The last step (formation of neutral **4c** and **3a**) would involve back electron transfer (BET) from $\mathbf{3a}^{\bullet-}$ to $\mathbf{4c}^{\bullet+}$.

In principle, the fate of the geminate radical ion pairs might be influenced by their spin multiplicity, inherited from that of the involved photosensitizer excited state. However, this does not seem to play an important role in the present case, as it has been demonstrated that cycloreversion occurs from the triplet excited state both with (thia)pyrylium ions and with chloranil.[20]

Thus, the CR pathway depends on the choice of the photosensitizer. Theoretical calculations confirm the proposed CR mechanism for oxetane radical cations generated by electron transfer and may be used to predict the reactivity of simple compounds. However, the possible interaction within the generated radical ion pair has to be taken into account to explain the actual reaction pathway.

Conclusions

As a conclusion, the present DFT study for the cycloreversion mechanism of oxetane radical cations supports a concerted but asynchronous process in which breaking of the C_3-C_4 bond at the TS is more advanced than that of the $O-C_2$ bond. This rearrangement allows a favorable redistribution of the spin electron density from the oxetane radical cation, where the spin density is located mainly on the oxygen atom, to the alkene radical cation. Inclusion of solvent effects does not modify the results obtained in the gas phase. These DFT results are in agreement with the observed regioselectivity for the cycloreversion of oxetanes using cyanoaromatics and chloranil as ET-photosensitizers. However, the opposite regioselectivity observed for the cycloreversion of **1c,d** photosensitized by (thia)pyrylium salts **3a,b** points to an initial $O-C_2$ bond breaking, as a consequence of an interaction of the pyranyl radical with the oxetane radical cation before fragmentation.

Acknowledgment. This work was supported by research funds provided by the Spanish Government (Projects BQU2001-2725 and BQU2002-01032) and the Generalitat Valenciana (Grupos 03/082 and 03/176). We are indebted to Dr. M. Lamsabhi for his assistance with the NRT calculations.

References and Notes

(1) Griesbeck, A. G. In *CRC Handbook of Organic Photochemistry and Photobiology*; Horspool, W. M., Song, P.-S., Eds.; CRC Press: Boca Raton, FL, 1995; pp 522−535.

(2) (a) Bach, T. *Synthesis* **1998**, 683−703. (b) Bach, T. *Liebigs Ann./Recl.* **1997**, 1627−1634. (c) Jones, G., II; Aquadro, M. A.; Carmody, M. A. *J. Chem. Soc., Chem. Commun.* **1975**, 206.

(3) (a) Zhao, X.; Liu, J.; Hsu, D. S.; Zhao, S.; Taylor, J. S.; Sancar, A. *J. Biol. Chem.* **1997**, *272*, 32580−32590. (b) Joseph, A.; Falvey, D. E. *Photochem. Photobiol. Sci.* **2002**, *1*, 632−635. (c) Cichon, M. K.; Arnold, S.; Carell, T. *Angew. Chem., Int. Ed.* **2002**, *41*, 767−770.

(4) Wang, Y.; Gaspar, P. P.; Taylor, J. S. *J. Am. Chem. Soc.* **2000**, *122*, 5510−5519.

(5) (a) Nakabayashi, K.; Kojima, J. I.; Tanabe, K.; Yasuda, M.; Shima, K. *Bull. Chem. Soc. Jpn.* **1989**, *62*, 96−101. (b) Prakash, G.; Falvey, D. E. *J. Am. Chem. Soc.* **1995**, *117*, 11375−11376.

(6) Miranda, M. A.; Izquierdo, M. A. *Photochem. Photobiol. Sci.* **2003**, *2*, 848−850.

(7) (a) Miranda, M. A.; Izquierdo, M. A.; Galindo, F. *J. Org. Chem.* **2002**, *67*, 4138−4142. (b) Miranda, M. A.; Izquierdo, M. A. *J. Am. Chem. Soc.* **2002**, *124*, 6532−6533.

(8) (a) Becke, A. D. *J. Chem. Phys.* **1993**, *98*, 5648−5652. (b) Lee, C.; Yang, W.; Parr, R. G. *Phys. Rev. B* **1988**, *37*, 785−789.

(9) Hehre, W. J.; Radom, L.; Schleyer, P. v. R.; Pople, J. A. *Ab initio Molecular Orbital Theory*; Wiley: New York, 1986.

(10) (a) Schlegel, H. B. *J. Comput. Chem.* **1982**, *3*, 214. (b) Schlegel, H. B. Geometry Optimization on Potential Energy Surface. In *Modern Electronic Structure Theory*; World Scientific: Singapore, 1994.

(11) Fukui, K. *J. Phys. Chem.* **1970**, *74*, 4161−4163.

(12) (a) González, C.; Schlegel, H. B. *J. Phys. Chem.* **1990**, *94*, 5523−5527. (b) González, C.; Schlegel, H. B. *J. Chem. Phys.* **1991**, *95*, 5853−5860.

(13) Reed, A. E.; Weinstock, R. B.; Weinhold, F. *J. Chem. Phys.* **1985**, *83*, 735−746.

(14) Frisch, M. J.; Trucks, G. W.; Schlegel, H. B.; Scuseria, G. E.; Robb, M. A.; Cheeseman, J. R.; Zakrzewski, V. G.; Montgomery, J. A., Jr.; Stratmann, R. E.; Burant, J. C.; Dapprich, S.; Millam, J. M.; Daniels, A. D.; Kudin, K. N.; Strain, M. C.; Farkas, O.; Tomasi, J.; Barone, V.; Cossi, M.; Cammi, R.; Mennucci, B.; Pomelli, C.; Adamo, C.; Clifford, S.; Ochterski, J.; Petersson, G. A.; Ayala, P. Y.; Cui, Q.; Morokuma, K.; Malick, D. K.; Rabuck, A. D.; Raghavachari, K.; Foresman, J. B.; Cioslowski, J.; Ortiz, J. V.; Stefanov, B. B.; Liu, G.; Liashenko, A.; Piskorz, P.; Komaromi, I.; Gomperts, R.; Martin, R. L.; Fox, D. J.; Keith, T.; Al-Laham, M. A.; Peng, C. Y.; Nanayakkara, A.; Gonzalez, C.; Challacombe, M.; Gill, P. M. W.; Johnson, B. G.; Chen, W.; Wong, M. W.; Andres, J. L.; Head-Gordon,

M.; Replogle, E. S.; Pople, J. A. *Gaussian 98*, revision A.6; Gaussian, Inc.: Pittsburgh, PA, 1998.

(15) (a) Tapia, O. *J. Math. Chem.* **1992**, *10*, 139−181. (b) Tomasi, J.; Persico, M. *Chem. Rev.* **1994**, *94*, 2027−2094. (c) Simkin, B. Y.; Sheikhet, I. *Quantum Chemical and Statistical Theory of Solutions-A Computational Approach*; Ellis Horwood: London, 1995.

(16) (a) Cances, M. T.; Mennunci, V.; Tomasi, J. *J. Chem. Phys.* **1997**, *107*, 3032−3041. (b) Cossi, M.; Barone, V.; Cammi, R.; Tomasi, J. *Chem. Phys. Lett.* **1996**, *255*, 327−335. (c) Barone, V.; Cossi, M.; Tomasi, J. *J. Comput. Chem.* **1998**, *19*, 404−417.

(17) Bader, R. F. W. *Atoms in Molecules. A Quantum Theory*; Oxford University Press: New York, 1990.

(18) Wiberg, K. B. *Tetrahedron* **1968**, *24*, 1083−1096.

(19) Glendening, E. D.; Badenhoop, J. K.; Reed, A. E.; Carpenter, J. E.; Bohmann, J. A.; Morales, C. M.; Weinhold, F. *NBO 5.0*; Theoretical Chemistry Institute, University of Wisconsin: Madison, WI, 2001.

(20) (a) Miranda, M. A.; Izquierdo, M. A.; Perez-Ruiz, R. *J. Phys. Chem. A* **2003**, *107*, 2478−2482. (b) Izquierdo, M. A.; Miranda, M. A. *Eur. J. Org. Chem*. **2004**, 1424−1431.